Supplementary Figure 3

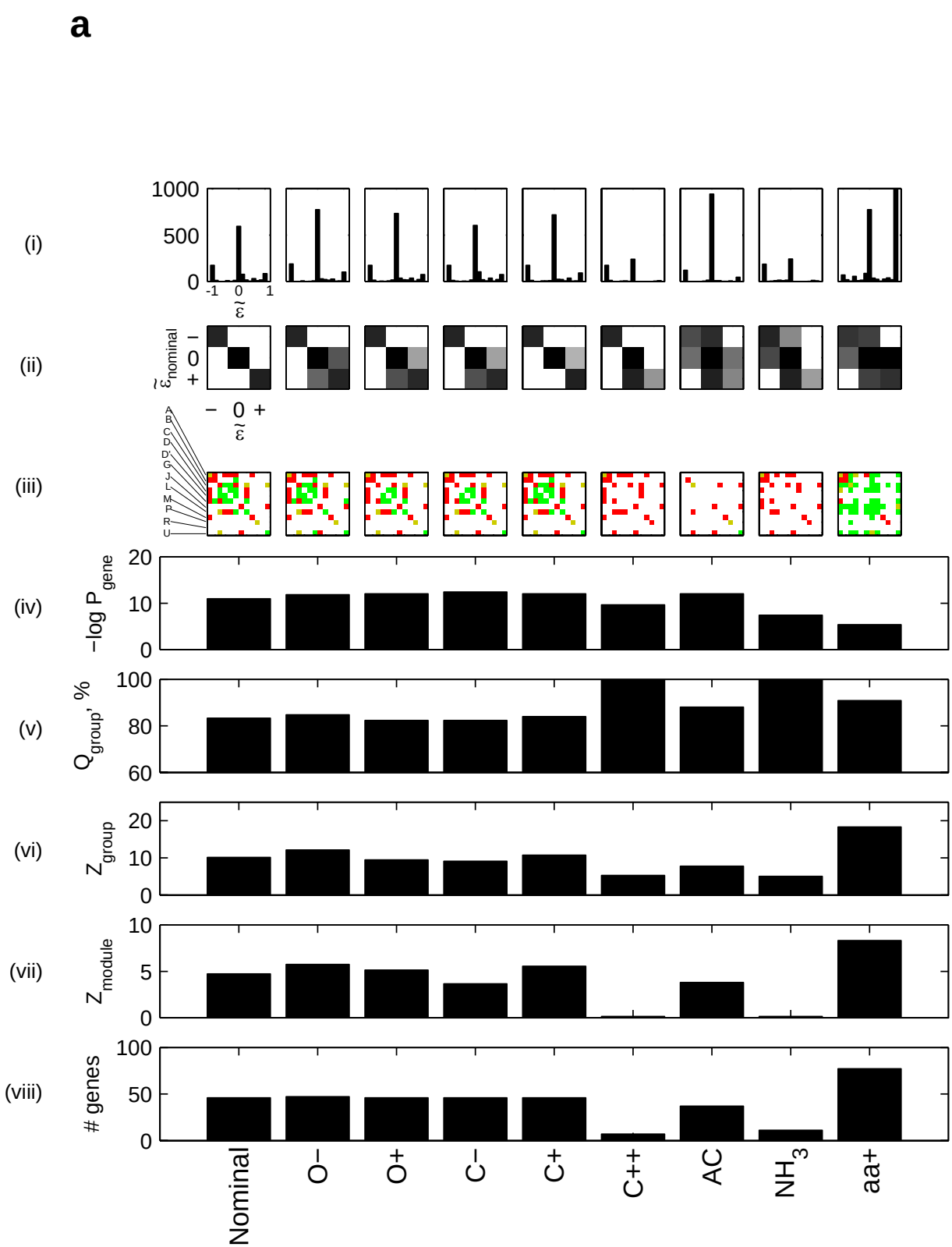

b

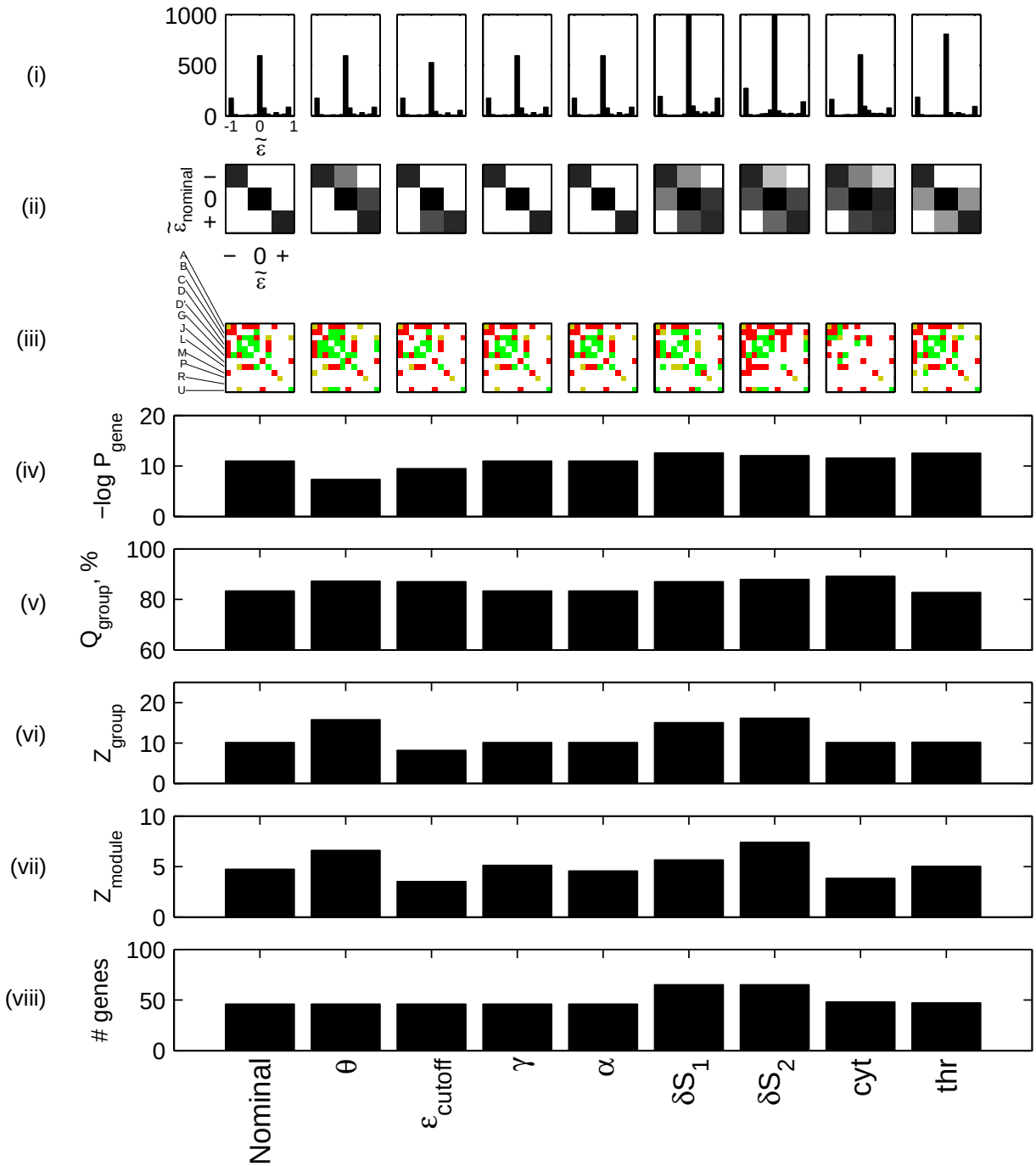
(i)
1000
500
0
-1 0 1
(ii)
(iii)
A
B
C
D
D'
G
J
L
M
P
R
U
(iv)
−log P gene
20
10
0
(v)
Q group, %
100
80
60
(vi)
Z group
20
10
0
(vii)
Z module
10
5
0
(viii)
genes
100
50
0
Nominal
θ
ε cutoff
γ
α
δS1
δS2
cyt
thr

Supplementary Fig. 3: Sensitivity analysis with respect to free parameters and physiological conditions. Several different outcomes (rows i-viii) of the model and data analysis are depicted for different settings of the free parameters in the FBA model and the Prism algorithm (columns). Overall, the main results and especially the properties of trimodality of the epistasis distribution and monochromaticity of the ensuing network seem to be robust with respect to most perturbations. Different rows, from top to bottom correspond to: (i) The distributions of the rescaled level of epistasis, $\tilde{\varepsilon}$, to be compared with **Fig. 1b**; (ii) A matrix describing the number of links that change category (- aggravating, 0 non-interacting, + buffering), when comparing nominal conditions (y axis) and the condition under exam (x axis); the gray scale (from white to black) is proportional to the logarithm of the number of links changing from one category to the other; (iii) A matrix showing the monochromaticity of the interactions between different annotation groups; the analysis is equivalent to that shown in **Fig. 2b**. Red, green and orange pixels correspond to purely aggravating, purely buffering, and mixed interactions, respectively; the classes shown constitute a selected subset of the complete set of annotations, visible in **Fig. 2a**; (iv) $-\log_{10} P_{gene}$, level of statistical significance for the enrichment of common annotation among pairs of genes that display an epistatic interaction (calculated using the hypergeometric distribution, see Methods); (v) Relative Q_{group} (%), percentage of all interacting annotation group pairs that interact monochromatically; this corresponds to the fraction of red or green pixels over total number of coloured pixels for the complete versions of the matrices in (iii) (off-diagonal only); (vi) Z_{group}, number of standard deviations between the number of non-monochromatic links Q_{group} of the actual epistatic network and the corresponding average for an ensemble of randomized networks (see Methods and **Supplementary Fig. 7c**). Larger values mean lower probability of obtaining the observed value by chance; (vii) Z_{module}, number of standard deviations describing the statistical significance of monochromatic clusterability with Prism. Large values, again, imply lower probability of obtaining the observed Q_{module} value by chance (See Methods and **Supplementary Fig.7d**); (viii) Number of genes with non-lethal finite effect on fitness, describing the overall extent of phenotypic perturbations relevant for studying epistasis.

Detailed descriptions of the conditions and perturbations applied for every different column can be found in **Supplementary Table 1**.

(a) Comparison of different physiological growth conditions. For the main limiting nutrients (i.e. the upper bounds for the uptake rates of oxygen and glucose), we perform positive and negative variations with respect to the nominal condition (O-, O+, C-, C+, C++, see **Supplementary Table 1**). In all cases, except the extreme perturbation C++, all statistical tests for monochromaticity are highly significant, and close to the values for the nominal condition. This can also be seen from the little changes in the matrices of row iii. While the epistasis distributions (row i) remain clearly trimodal, only through the matrices of row ii it is possible to appreciate whether links changed color, and in what way. In particular, it can be seen that while most links maintained their original nature (black diagonal blocks), all changes with respect to the nominal condition involved transitions from buffering to non-interacting and vice versa. By examining all matrices on row ii (both here and in **Supplementary Figs. 3b**), one can see that it is extremely unlikely to observe a transition of a red link becoming green (or vice versa), even with drastic changes of conditions or statistical parameters. When glucose is increased to saturation level, and stops being the limiting resource (C++) the number of genes with finite fitness effect drops down (row viii), substantially reducing the number of detectable buffering interactions (rows i, iii). This is due to the artificial scenario, occurring in C++, in which respiratory metabolism, where many of the buffering links are formed, does not contribute to energy generation, and thus deletions of these genes no longer have an effect on fitness. A similar situation is observed when nitrogen, not carbon, is the limiting resource. Note however that the aggravating interactions remain mostly unchanged with respect to the nominal case (row iii). The 100% presence in monochromatically linked annotation groups (row v) is an obvious consequence of the small number of genes displaying non-trivial phenotypes, and the overall abundance of aggravating interactions, and it is therefore much less significant (row iv and vii).

Among the other conditions analyzed, the acetate medium (AC) and the amino-acid supplemented medium (aa+) deserve special attention. In both cases, an abundant number of interactions transform from aggravating or buffering to no-epistasis (and vice-

versa) (rows ii and iii). This is especially evident in aa+, where a large number of buffering interactions in the amino acid metabolism annotation groups appear. This can be rationalized by the fact that when amino acids are provided and two of them become essential in the double auxotroph, the one which is most limiting would determine the growth. While this result may significantly depend on the absence of regulatory information in the FBA model, it points again to possible ways of tuning the relative amounts of buffering and aggravating interactions measurable under a given condition. In the opposite example, several buffering links are lost when acetate, a non-fermentable carbon source, is used instead of glucose. Here, buffering links with genes of the respiratory metabolism cannot be formed given that these genes become lethal when energy is exclusively generated through respiratory metabolism.

These results suggest that preliminary computational studies under several different conditions may help design optimal experiments that would give large and balanced numbers of aggravating and buffering interactions. Since different genes are shown to be observed under different conditions, optimal design criteria of this kind could be extended to high-throughput multiple conditions experiments. In addition, one could speculate that such condition-dependent variability in the number of interactions that "light up" could support the dependence of epistasis on environmental conditions suggested and reported in experimental setups [36,37].

(b) The first half of the sensitivity analyses columns in this panel relate to post-FBA analysis of the data (see **Supplementary Table 1**): θ - for changes in the $\tilde{\varepsilon}$ thresholds defining the type of interaction for each pair of genes; ε_{cutoff} - for the level of noise filtered out when generating the $\tilde{\varepsilon}$ distribution (defined in **Table 1**); α and γ - for changes in the values of the parameters defining the cluster-cluster affinities in the Prism algorithm (see Methods).

The second half of the columns in this panel shows the result of additional modifications in FBA constraints: δS_1 and δS_2 correspond to different kinds of random perturbations applied to the stoichiometric matrices (**Supplementary Table 1**). In the *cyt* and *thr* columns, single constraints present in the nominal settings were reversed (*cyt* was

set to unbound, and *thr* to zero, respectively, see Supplementary Methods and **Supplementary Table 1**).

The robustness columns related to the post-FBA analysis all display the same number of significant genes (row viii), simply because they all refer to the same nominal data set. The sensitivity for the threshold values θ emphasizes the relevance of the trimodal distribution in defining the epistatic network. As seen in row ii, this perturbation decreases the number of links considered red, and increases the number of links considered green. From row iii it is possible to see some examples of how these changes affect the interaction at the level of annotation groups. Thus, a new set of pure buffering interactions appear between genes of the pentose phosphate pathway and the respiratory chain, which is sound given the NADP coupling of these processes by the activity of the *NCP1*-encoded oxidase in a *rip1*Δ background (see groups labeled B, D, D'). However, the mild cutoff for green links would certainly lead to artifacts such as the ensuing buffering interaction between ATP synthetase and tryptophan catabolism genes (see groups G, J). In a different example, monochromaticity is violated when the lenient cutoff value (θ_+=0.5 compared to 0.9 in the nominal case) allows buffering links between glycolysis and the anaplerotic reactions, which in the nominal analysis are conected exclusively by aggravating links (see groups A, H). While statistical significance levels are mildly affected by this perturbation, they don't affect the overall conclusion of monochromatic nature of modular organization. It should be noted that a less sharply trimodal distribution could have produced much more dramatic effect under this θ perturbation. The increased stringency of the noise filtering level analyzed in the ε_{cutoff} column has a somewhat opposite effect, in the sense that it reduces the number of links considered buffering. Note however, that while a change of θ only affects the choice of links on the network, a change in ε_{cutoff} affects the distribution of $\tilde{\varepsilon}$ itself. The balance between these two parameters may be very useful for defining an optimal ratio of true positives to false positives in the interpretation of experimental data.

By definition, changes in α and γ can only affect outcomes of the Prism clustering solution, and will be reflected only in the Z_{module} graph (row vii). As seen, the significance level of a monochromatic Prism solution, is hardly affected by changing α from 0.3 to 1 or γ from 100 to 1 (this is true also in the extreme case of α=0; data not shown). This is

basically a consequence of the fact that the monochromatic clusterability of the yeast epistatic network is an intrinsic property of the network, largely independent of the specific algorithm used to achieve it (see Prism-R and corresponding P-value in the Methods). Importantly, however, the specific details of clustered modules can be affected by α. A noticeable example is the splitting of the acetaldehyde and ethanol metabolism module (see box labeled *ACAL* in **Fig. 4a**) into two separate modules – one of them merged with the respiratory chain – when changing the value of α to 0 from 0.3. After this change, only direct interactions are considered for clustering affinities (see Methods). Thus, it is to be expected that modules with highly connected genes, such as those for acetyl-CoA and pyruvate metabolism, will be prone to be reorganized after changes in the clustering parameters. In this way, different α values can be used when trying to give emphasis on direct rather than associative interactions (i.e. similar links to other genes), or vice versa. High values of γ can be used to put emphasis on associative similarity effects in the lower clustering levels and on direct connections in the higher module-module levels. In the nominal analyses, we used γ=100. An extreme change to γ=1 produces a similar allocation to modules, except for proline catabolism genes which are clustered together with respiratory chain genes.

The analysis of randomized stoichiometric matrices (columns δS_1 and δS_2, **Supplementary Table 1**) constitutes the initial stage of a possibly much deeper and more complex direction of research. While the simple method of randomization chosen here modifies by 50% a small proportion of nonzero stoichiometric coefficients (δS_1), or switches to –1 or 1 a small proportion of zero coefficients (δS_2), more elaborated randomization schemes may be designed, that do not change overall elemental balance. The results presented here indicate that such random perturbations have an unexpectedly small effect both on the statistical significance levels, and on the specific details of annotation group interactions (row iii). It will be interesting to study to what extent the analysis of epistatic network modules based on phenomenological studies will allow to identify possible mistakes in our current understanding of biochemical pathways, and in the recovery of the “true” networks.

Minor effects on the levels of statistical significance are observed in the *cyt* and *thr* perturbations. The reintroduction of full respiratory capacity caused by allowing

cytochrome c reductase activity (*cyt*) is reflected in the disappearance of a block of buffering interactions mainly composed of carbon metabolism genes (respiratory chain, ATP synthetase, pyruvate metabolism, and pentose phosphate pathway). In an optimized model, an intact respiratory chain will primarily direct the flux of carbon through oxidative phosphorilation, and thus will increase the fitness contribution of the genes for respiration. Accordingly, synergistic interactions of respiration and ATP synthetase with glycolysis are maintained, but many of their buffering links with other modules are lost and now have a neutral multiplicative effect (see example below).

(For references, see **Supplementary References** online)